

Geophysical Research Letters*



RESEARCH LETTER

10.1029/2023GL103632

Key Points:

- Provenance changes at the outlet of the Hetao Basin indicate the desiccation and re-integration of the upper Yellow River over the last ~40 ka
- Paleo-lake shorelines and geochemical proxies confirm that the west Hetao Basin contained the terminal lake for the desiccated Yellow River
- Climate-river feedbacks across glacial-interglacial cycles have implications for constraining terrestrial-marine source-to-sink processes

Supporting Information:

Supporting Information may be found in the online version of this article.

Correspondence to:

N. Fan, fannianian@scu.edu.cn

Citation:

Zhao, Y., Fan, N., Nie, J., Abell, J. T., An, Y., Jin, Z., et al. (2023). From desiccation to re-integration of the Yellow River since the last glaciation. *Geophysical Research Letters*, 50, e2023GL103632. https://doi.org/10.1029/2023GL103632

Received 15 MAR 2023 Accepted 12 JUL 2023

Author Contributions:

Conceptualization: Niannian Fan, Junsheng Nie, Jordan T. Abell Data curation: Yuqi Zhao, Niannian Fan, Jiafu Zhang

Formal analysis: Yuqi Zhao, Niannian Fan, Junsheng Nie

Funding acquisition: Niannian Fan, Zhangdong Jin, Chengshan Wang Investigation: Yuqi Zhao, Niannian Fan, Yu An

Methodology: Yuqi Zhao, Niannian Fan, Yu An

Project Administration: Niannian Fan **Resources:** Yuqi Zhao, Niannian Fan

© 2023. The Authors.

This is an open access article under the terms of the Creative Commons Attribution License, which permits use, distribution and reproduction in any medium, provided the original work is properly cited.

From Desiccation to Re-Integration of the Yellow River Since the Last Glaciation

Yuqi Zhao¹, Niannian Fan^{1,2}, Junsheng Nie³, Jordan T. Abell⁴, Yu An^{1,5}, Zhangdong Jin², Chengshan Wang⁶, Jiafu Zhang⁷, Xingnian Liu¹, and Ruihua Nie¹

¹State Key Laboratory of Hydraulics and Mountain River Engineering, College of Water Resource & Hydropower, Sichuan University, Chengdu, China, ²State Key Laboratory of Loess and Quaternary Geology, Institute of Earth Environment, Chinese Academy of Sciences, Xi'an, China, ³MOE Key Laboratory of Western China's Environment Systems, College of Earth and Environmental Sciences, Lanzhou University, Lanzhou, China, ⁴Department of Geosciences, University of Arizona, Tucson, AZ, USA, ⁵Planning & Development Research Division, Northwest Engineering Corporation Limited, Xi'an, China, ⁶State Key Laboratory of Biogeology & Environment Geology College of Earth Sciences, China University of Geosciences (Beijing), Beijing, China, ⁷MOE Laboratory for Earth Surface Processes, College of Urban and Environmental Sciences, Peking University, Beijing, China

Abstract The desiccation (extreme drying) of rivers has important implications for the broader Earth System. However, the desiccation history and its linkage to climate are rarely known for numerous major river systems, primarily due to difficulties in recognizing desiccation events from available stratigraphic records. Here, using a combination of geochemical techniques (major and rare-earth element geochemistry, detrital zircon geochronology, and optically stimulated luminescence dating), we demonstrate that the Yellow River, which maintains the highest sediment load on Earth, became desiccated during the Last Glacial Maximum at approximately 20 thousand years ago. This finding implies that transportation of sediments and dissolved constituents to the oceans via the Yellow River may have decreased substantially or ceased during glacials, which would have ramifications for ocean chemistry and biology. Furthermore, our work highlights the importance of desiccated riverbed sediments as potential dust sources during glacial periods, a finding that is different from what is observed today.

Plain Language Summary Understanding the characteristics of major rivers is important for better constraining changes in the Earth System. Based on new geochemical data, we find that during the period dominated by overall drier and colder climate conditions ~20,000 years ago, water flow in the upper reaches of the Yellow River was reduced to the point that flow effectively ceased downstream of the Hetao Basin. In other words, the Yellow River was no longer a perennial river between the upper and middle-low reaches until re-integrating ~10,000–5,000 years ago. Moreover, we demonstrate that surface processes related to the Yellow River system are substantially different between colder-drier and warmer-wetter intervals, at least for the last ~40 thousand years, and we suggest caution when using modern observations to infer regional environments and geomorphology related to rivers during colder-drier periods.

1. Introduction

Rivers are key components of the Earth System; they can modify regional landscapes, transport material from land to the oceans, and are relevant for various regional and global climate feedback systems. However, in contrast to river flooding, the characteristics of which (e.g., event frequency and underlying drivers) have been extensively studied (T. Li et al., 2020; Ma et al., 2022; S. Yu et al., 2020), much less is known regarding the desiccation history of rivers, its relationship with regional and global climate, and the overall impact on local landscapes.

One example of this discrepancy in knowledge is the Yellow River, which contains the highest sediment load on the planet, transporting over 1 billion tons of sediment annually (Ma et al., 2022). Much of the available literature related to this river system focuses on the age of its formation (Hu et al., 2017; X. Wang et al., 2022), flooding history (T. Li et al., 2020), and morphology (Jia et al., 2016; Tang et al., 2023), but there is a dearth of work exploring the Yellow River's desiccation history and the underlying mechanisms driving the drying (Xia et al., 1996).

ZHAO ET AL. 1 of 12



Geophysical Research Letters

10.1029/2023GL103632

Software: Yuqi Zhao, Niannian Fan Supervision: Niannian Fan Validation: Yuqi Zhao, Niannian Fan Visualization: Niannian Fan Writing – original draft: Yuqi Zhao, Niannian Fan, Junsheng Nie, Jordan T. Abell

Writing – review & editing: Yuqi Zhao, Niannian Fan, Junsheng Nie, Jordan T. Abell, Zhangdong Jin, Chengshan Wang, Jiafu Zhang. Xingnian Liu. Ruihua Nie River terrace sequences mark a river's course through its geological history. Importantly, the detrital zircons in these deposits are derived from the various source terranes, and contain the geological age signatures of these source rocks. These conditions make terraces ideal for studying river evolution through time. For the Yellow River in particular, a series of alluvial terraces developed in the Hequ area (J. Zhang et al., 2009), the first intermontane basin downstream of the Hetao Basin (Figure 1b).

Here, we use optically stimulated luminescence (OSL) dating and detrital zircon geochronology from these terraces in the Hequ area (Figure 1c) to reconstruct the late Quaternary provenance history of the Yellow River. Combining this information with previous work (Fan et al., 2010, 2022; Nie et al., 2015; J. Zhang et al., 2009; M. Zhang, Liu, Yu, & Wang, 2022), we then infer the desiccation history of the Yellow River, specifically demonstrating for the first time that during the Last Glacial Maximum (LGM) ~20 thousand years ago (ka), perennial flow ceased, and the upper reaches of the Yellow River terminated in a paleo-lake in the western Hetao Basin (Figure 1b), with flow eventually resuming during the Holocene. Finally, we evaluate this desiccation event with respect to climate as well as its impact on regional geomorphology in the middle reaches of the Yellow River over the last ~40 ka.

2. Materials and Methods

2.1. Fluvial Sediment Sampling

The Hequ area is located at the periphery of the Ordos Block (Figure S1 in Supporting Information S1), which consists of Archean-Paleoproterozoic metamorphic crystalline basement and subsequent Meso-Neoproterozoic to Meso-Cenozoic sedimentary cover (Z. Wang et al., 2015). Clastic deposits formed sporadically around the Hequ area from Carboniferous to Quaternary outcrops (Figure S2 in Supporting Information S1).

Samples from four terraces (A, C, D, and H') and one modern riverbed sample were taken from the Hequ area (Text S2 and Table S4 in Supporting Information S1). The formation ages of the terraces, determined using the OSL dating method, are 5.1 ± 0.5 (2σ), 10.1 ± 0.6 , 20.3 ± 2.0 , and 37.1 ± 2.3 ka, respectively (J. Zhang et al., 2009) (Table S2 in Supporting Information S1). We also sampled fluvial sediments from various tributaries (such as the Gushan River) in the upper section of Jinshaan Gorge for comparison (Figure S3 in Supporting Information S1).

2.2. Optically Stimulated Luminescence Dating

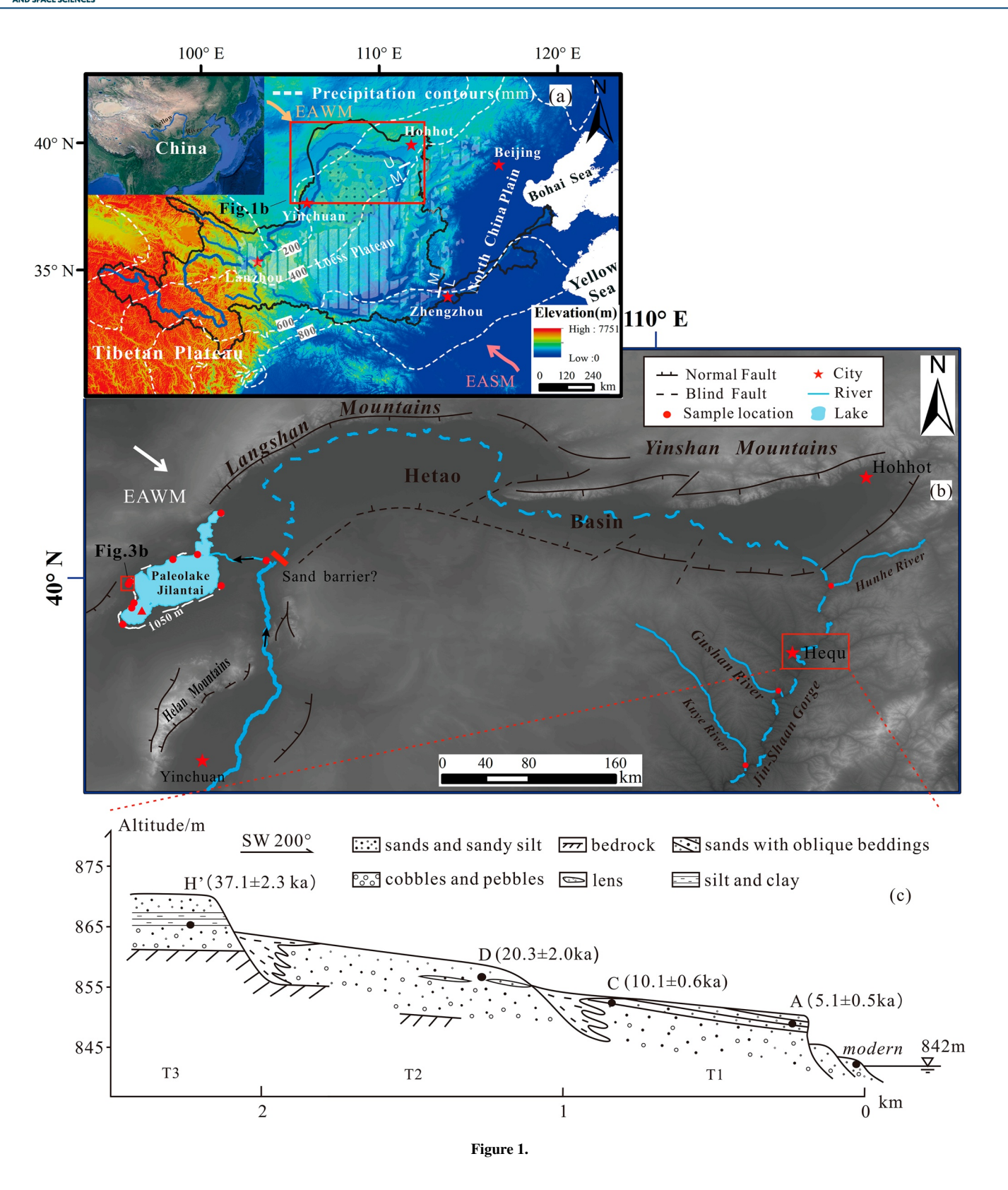
The sample preparation and OSL measurements on quartz and K-feldspar fractions were conducted in the luminescence dating laboratory at Linyi University. A preheat of 260°C for 10 s, 220°C cutheat temperature, 5°C s⁻¹ heating rate and a one-third measuring dose for the test dose were used in all dose measurements. For samples with saturated quartz OSL signals (saturation dose of ca. ~120–150 Gy in some cases (Buylaert et al., 2008)), K-feldspar OSL signals were measured. K-feldspar dating utilizes the Infrared Radiation Stimulated Luminescence signal obtained from progressively increasing the stimulation temperature from 110°C to 170°C in step of 30°C (see Figure S4 in Supporting Information S1). The doses could be recovered under the stimulation temperature of 140°C–170°C for the samples in this study, and the concentrated D_e and low over dispersion (OD) values further suggest bleaching of pIRIR signals (see Table S1 in Supporting Information S1). For OD values \leq 23% or >23% of the dose values, central age model and minimum age model were used to calculate the equivalent dose, respectively (Medialdea et al., 2014) (Table S1 in Supporting Information S1).

2.3. Major and Rare-Earth Elements

The pre-treated sediments were measured on an Agilent 7900 ICP-MS (for details see Table S5 in Supporting Information S1) to acquire rare-earth element concentrations. Each sample was scanned five times, and the analytical precision is better than 5% 1RSD (relative standard deviation). Major element concentrations were determined by X-ray fluorescence spectrometry using an Axios^{MAX} XRF at Nanjing Hongchuang Exploration Technology Service Co., Ltd. In order to monitor the impacts of chemical pre-treatment and matrix effects on our measurements, each batch of samples was analyzed in parallel with several sediment standards (andesite AGV-2, GBW07103, etc.; see Dataset S2). The reproducibility of all major and rare-earth element results was determined via rock standard samples, and was guaranteed to be less than $\pm 10\%$ for rare-earth elements and less than $\pm 5\%$ for major elements.

ZHAO ET AL. 2 of 12

from https://agupubs.onlinelibrary.wiley.com/doi/10.1029/2023GL103632 by University Of Arizona Library, Wiley Online Library on [09/08/2023]. See the Terms and Conditions (https://onlinelibrary.wiley.com/errns



2.4. U-Pb Ages of Detrital Zircons

Nine fluvial deposits were sampled and more than 1,000 zircon grains were extracted from up to 1 kg samples for each sample. First, the samples were treated by magnetic separation, and for the nonmagnetic portion,

ZHAO ET AL. 3 of 12

conventional elutriation separation was used to obtain zircon grains. Then ~ 150 grains were randomly picked under a binocular microscope, mounted on a double-sided tape, caste in epoxy resin, and finally polished to expose surfaces for Laser Ablation-Inductively Coupled Plasma-Mass Spectrometry analysis. The laser-beam diameter was 30 μ m with a 5 Hz repetition rate and energy of 2–3 J/cm². Fifteen percent discordance filter to the generated data was applied, and we used $^{206}\text{Pb}/^{238}\text{U}$ ages for zircon grains younger than 1,000 Ma and $^{207}\text{Pb}/^{206}\text{Pb}$ ages for grains older than 1,000 Ma (Y. Chen et al., 2017). Cathodoluminesce (CL) imaging was undertaken to reveal internal structures, both the core and rim parts of the zircon grains were analyzed (see Text S6 and Figure S5 in Supporting Information S1 for more details).

3. Results

3.1. Sediment Provenance Changes in the Hequ Area

Detrital zircon age distributions for the fluvial deposits of Hequ-modern, Hequ-A, and Hequ-H' are different from those of Hequ-C and Hequ-D (Figure 2). The detrital zircons of both Hequ-D and Hequ-C have similar age spectra, with ages clustering around 1,800 and 2,500 Ma, as does the local tributary (i.e., the Gushan River) (Figures 2a5–2a7), which correspond to the Lyliang (1,700–1,900 Ma) and Wutai (2,300–2,600 Ma) Orogenies, respectively (see Text S1 in Supporting Information S1). Additionally, samples Hequ-D and Hequ-C have fewer (<2%) detrital zircons with ages of ~800–1,000 Ma derived from the Songpan-Garze Flysch at the source area of the Yellow River (Figures S1 and S6 in Supporting Information S1), and instead have predominant (58%–70%) contribution from proximal sources (the Neoarchean-Mesoproterozoic rocks, see Figure 2a7). Opposingly, Hequ-modern, Hequ-A and Hequ-H' display age spectra that are distributed more evenly (e.g., Indosinian [190–300 Ma], Jinning [800–1,000 Ma], Lyliang and Wutai Orogenies [Wu et al., 2020]), which correspond to multiple sediment sources, similar to the upper reaches of the modern Yellow River (Figures 2a1–2a2).

4. Discussion and Conclusion

4.1. Desiccation of the Yellow River During the LGM

The differences observed in detrital zircons age modes suggest changing the provenance of the Hequ terrace samples from distal to proximal sources during \sim 40–20 ka. This conclusion is also generally supported by distinct clustering of these samples based on (a) the multi-dimensional scaling (MDS) technique (Figure 2b), (b) rare-earth and major element data (Figures 2c and 2d), and (c) quantitative mixing models (Figures 2e and 2f) (Sundell & Saylor, 2017) for these detrital geochronology data.

The potential dust sources in the Hequ area may include sand from the Mu Us desert, aeolian loess, local bedrock, and the fluvial sediments in the upper Yellow River drainage system (Figure 1). Contributions from the Gobi deserts further to the north are likely represented by the Mu Us sand and the aeolian loess (Amit et al., 2014). The results of the Monte Carlo mixture model (Sundell & Saylor, 2017) suggest a significant shift of the dominant provenance from sample Hequ-D (Figure 2e) to sample Hequ-modern (Figure 2f), indicating the limited contributions of the upper Yellow River while proximal sources prevailed during \sim 20 ka.

The predominantly proximal provenance for samples Hequ-C and D during \sim 20–10 ka can be interpreted as: (a) river desiccation resulted in decreased input of distal provenance from the upper reaches of the Yellow River, or (b) increased local provenance input without river desiccation. We argue that the former interpretation is more likely. The period of approximately 20–10 ka corresponds to the LGM and subsequent deglacial period. Over this interval, the regional climate was generally drier than both the preceding \sim 100 ka and the Holocene Epoch that followed (Hou et al., 2021; McGee D., 2020; Yan & Bernd, 2014). During this time, the Yellow River would have

Figure 1. Climatic and tectonic characteristics of the study area. (a) Elevation and mean annual precipitation in the Yellow River drainage area. Dashed white lines denote precipitation contours. The loess-covered region is marked with a light-gray overlay. EASM, East Asian summer monsoon. The upper (U), middle (M), and lower (L) reaches of the Yellow River are delineated by solid white lines. The black solid line denotes the Yellow River drainage boundary. The inset map (from *Google Earth*) shows the location of the Yellow River in East Asia. (b) Schematic overview of the desiccation of the Yellow River and the paleo-Lake Jilantai during the last glacial period. The extent of the paleo-Lake Jilantai was reconstructed considering crustal flexural deformation (see Text S4 in Supporting Information S1 for details). Red dots show the location of outcrop samples. The triangle is a drill hole from M. Zhang, Liu, Yu, and Wang (2022). The red line is a possible sand barrier. EAWM, East Asian winter monsoon. (c) Schematic section of the Yellow River terraces in the Hequ area (modified from J. Zhang et al., 2009), showing the sample locations (Hequ-H', Hequ-D, Hequ-C, Hequ-A, Hequ-modern) and their respective ages. The slope deposits and colluvial deposits interfinger with the alluvium at the trailing edge of the lowest terrace (T1) and terrace T2.

ZHAO ET AL. 4 of 12

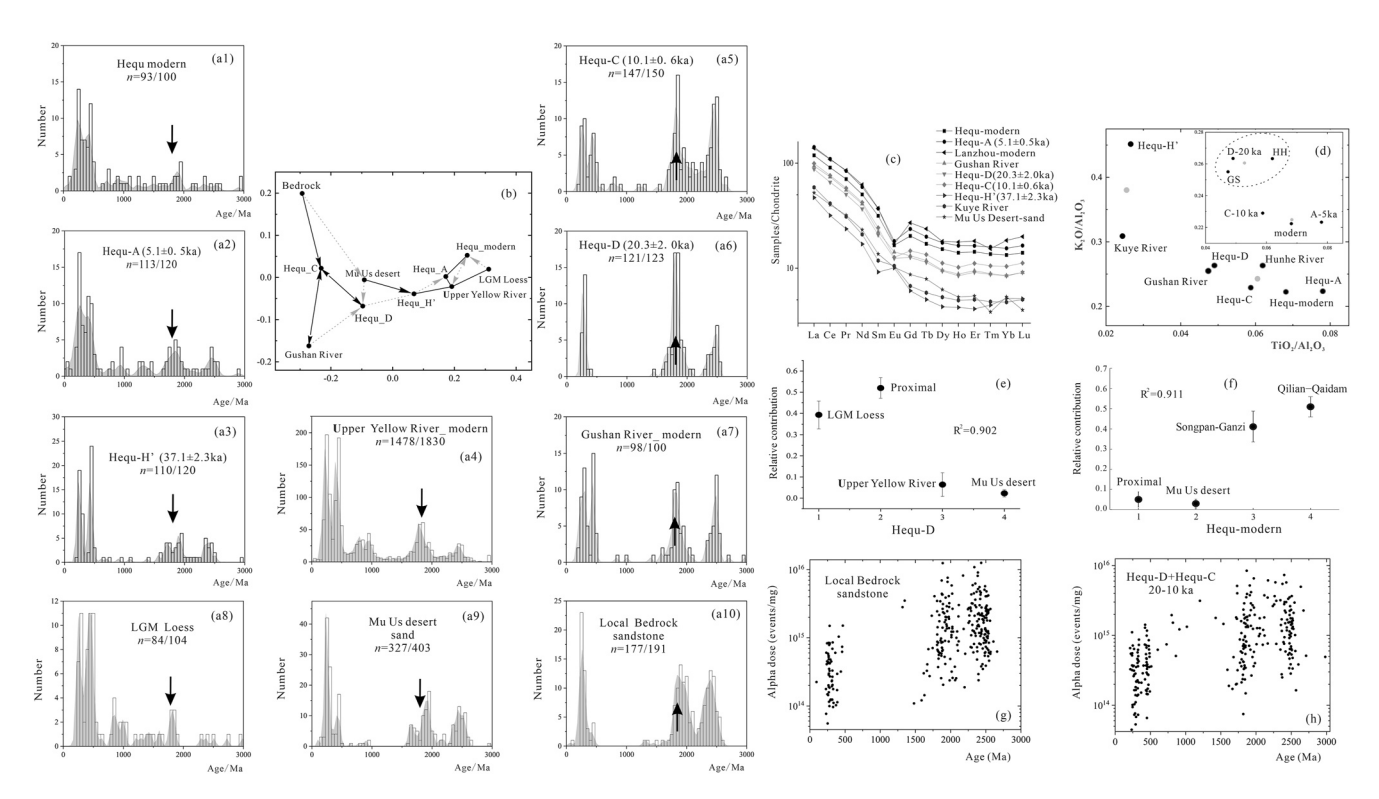


Figure 2. Geochemical indicators for terrace sediment provenance in Hequ area. (a1–a7) Detrital zircon U-Pb ages of fluvial deposits from the upper (data from Nie et al., 2015) and middle reaches of the Yellow River. Shaded areas are kernel density estimation plots, and the open rectangles are age histograms. *n* = total concordant analyses/total number of analyses. The arrows highlight the variable contributions of the zircons aged 1,700 to 1,900 Ma. (a8–a10) Detrital zircon U-Pb ages of the potential dust sources. The Last Glacial Maximum (LGM) loess data are from Stevens et al. (2010). The Mu Us desert sand data are from Licht et al. (2016), Nie et al. (2015), and Stevens et al. (2013). The local bedrock (sandstone) samples derived from the western Hequ area, are from Stevens et al. (2013). (b) A two-dimensional multi-dimensional scaling plot for detrital zircon U-Pb data of the study sites gives a quantitative comparison of similarities (Saylor et al., 2018). The final "stress" value was 0.053, which indicates a good fit (Kruskal et al., 1964). Axes are in dimensionless "K-S units" of the distance between samples. Solid lines and dashed lines mark the closest neighbors and the second closest neighbors, respectively. (c) Chondrite-normalized rare-earth element patterns for the studied samples. The elemental data from Lanzhou are from Pang et al. (2018), and the data from the Mu Us desert sand are from Lee et al. (2010). (d) Scatterplot of sample major elements ratios (TiO₂/Al₂O₃ and K₂O/Al₂O₃). The inset focuses on one of the clusters, and the gray dots are the clustering centers of each groups. GS, Gushan River; HH, Hunhe River (for zircon age mode, see Figure S3 in Supporting Information S1). (e–f) Quantitative mixing model results (Monte Carlo mixture modeling) for detrital geochronology data. The relative contribution of potential source samples to sample Hequ-D (e) and sample Hequ-modern (f) valued by the cross-correlation coefficient. (g–h) Plot of α-dose values (Dröllner et al., 2022) ver

experienced weakened water discharge, which would have resulted in lower input of sediment derived from the distal upper reaches of the river. Opposingly, the latter interpretation of increased proximal input would require more local runoff from enhanced precipitation, which is unlikely to occur over the generally drier period of \sim 20–10 ka (S. Yu et al., 2017). Additionally, zircon crystals separated from sample Hequ-D have a long columnar or subangular morphology (Figure S5 in Supporting Information S1), suggesting relatively short transport distances. Furthermore, the α -dose metric (α -decay events/mg) for individual zircon grains was used to evaluate the effect of sedimentary recycling on zircon data (Dröllner et al., 2022) (Figures 2g and 2h). There is no significant difference between the local bedrock and the fluvial samples aged \sim 20–10 ka (Hequ-D and Hequ-C) on the main ranges of zircon α -dose values, which means the radiation-damage related bias of the samples Hequ-D and Hequ-C is relatively minor, consistent with a first-cycle origin. Finally, the normal fault in the Hequ area has been inactive since the Pliocene (G. Liang et al., 2015), suggesting that the deformation and fragmentation processes induced by tectonic displacement were negligible (Andersen et al., 2022).

Detrital zircon ages of Hequ-H' $(37.1 \pm 2.3 \text{ ka})$ also suggest that the Yellow River was integrated prior to the LGM, as this sample displays a lower contribution of ages corresponding to proximal sources. However, we do note that the major and rare-earth element data indicate sample Hequ-H' is distinct from the two groups derived from detrital zircon ages alone (Figures 2c and 2d). We infer that the disparity in major and rare-earth elements may be related to the aeolian sand input from the Mu Us desert, which contains more mica/feldspar (potassium-bearing minerals) (Qian et al., 1993; R. Zhang et al., 2014), while riverbed sediments from the upper

ZHAO ET AL. 5 of 12

19448007, 2023, 15, Downloaded from https://agupubs.onlinelibrary.wiley.com/doi/10.1029/2023GL103632.by University Of Arizona Library, Wiley Online Library on [09/08/2023]. See the Terms and Conditions

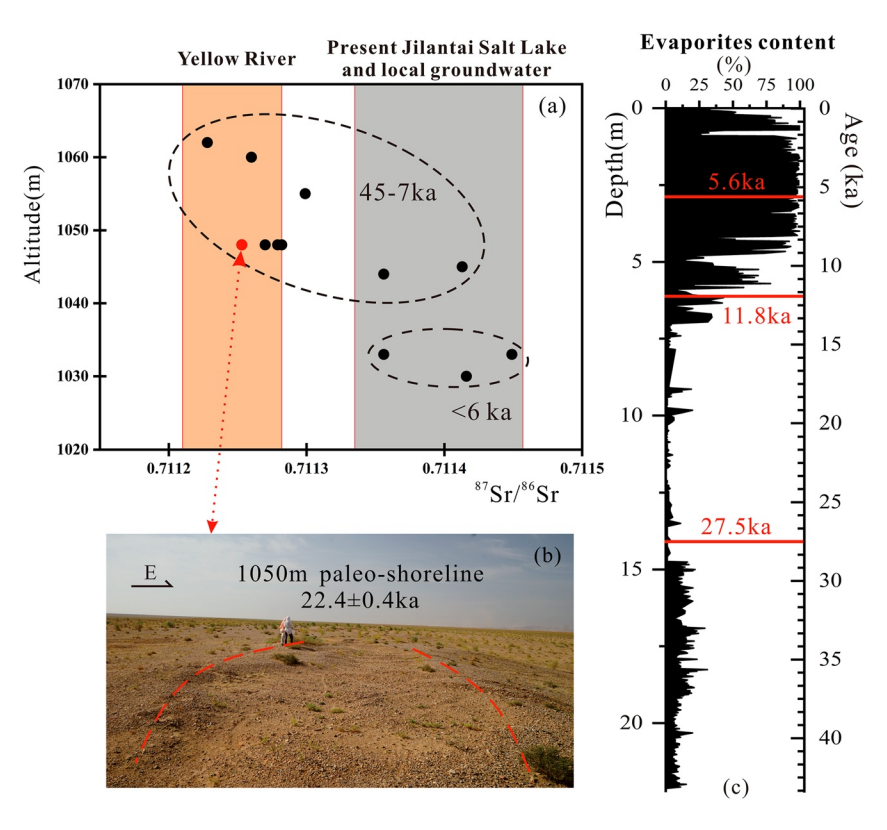


Figure 3. Sedimentary characteristics in the Jilantai area: (a) ⁸⁷Sr/⁸⁶Sr ratios of aquatic mollusk shells embedded in the relict shorelines versus present altitudes (Fan et al., 2010) and the age ranges. The red dot corresponds to the paleo-shoreline in subplot (b). The yellow bar shows the ⁸⁷Sr/⁸⁶Sr ratios of water from the Yellow River, and the gray bar indicates the water from the present Jilantai Salt Lake and local groundwater. (b) Photo of the paleo-lake shoreline during the Last Glacial Maximum, which is ∼30 m higher than the current water level. See Text S3 in Supporting Information S1 for more information about the paleo-lake shorelines and dating results. (c) The evaporite content (summation of Halite, Gypsum, Glauberite, Mirabilite and Bloedite) and ages of the core in the Jilantai Salt Lake from M. Zhang, Liu, Yu, & Wang (2022).

Yellow River are depleted in potassium (Pang et al., 2018). The upper reaches of the Kuye River flow through the southeastern margin of the Mu Us desert (Figure 1), and we find that the Kuye River sample clusters with the Hequ-H' sample in rare-earth and major element space. This observation supports our hypothesis regarding the input of detrital material from the Mu Us desert to the Hequ area around ~ 37 ka. Regardless, we suggest that the main course of the Yellow River remained integrated during this period.

4.2. The Terminal Lake for the Desiccated Yellow River in the Jilantai Area

Past desiccations of the Yellow River are not only evidenced by the terraces of the Hequ site studied here. Farther upstream of the modern Yellow River in the western Hetao Basin (Figure 1b), referred to as the Jilantai area, several paleo-shorelines are well preserved, which provide convincing evidence for lake formation, and in turn river desiccation, around 30–10 ka. Today, the Jilantai Salt Lake is not fed by the upper Yellow River. As a result, the ⁸⁷Sr/⁸⁶Sr ratio of the saline lake waters is close to that of the local groundwater, which is higher than the value for modern Yellow River waters (Figure 3a). However, ⁸⁷Sr/⁸⁶Sr ratios of aquatic mollusk shells imbedded in the paleo-shorelines show distinct ranges that vary with altitude (i.e., paleo-lake level) (Fan et al., 2010). Specifically, ⁸⁷Sr/⁸⁶Sr ratios of periods representing high lake levels are closer to that of the modern Yellow River, while increased ⁸⁷Sr/⁸⁶Sr values (similar to local groundwater) correspond to periods of lake lowstands. The ⁸⁷Sr/⁸⁶Sr ratios provide crucial evidence that the Yellow River was the dominant water source for the paleo-Lake Jilantai during the last glacial period when water levels were increased (Figure 3a and Table S1 in Supporting Information S1). Fluctuations in evaporite content from a drill hole suggest that the paleo-Lake Jilantai remained saline during the last 40 ka (M. Zhang, Liu, Yu, & Wang, 2022). However, during the cold, dry period spanning ~27.5–11.8 ka, the evaporite data implies that lower lake water salinity corresponded with intensified aeolian

ZHAO ET AL. 6 of 12

19448007, 2023, 15, Downloaded from https://agupubs.onlinelibrary.wiley.com/doi/10.1029/2023GL103632 by University Of Arizona Library, Wiley Online Library on [09/08/2023]. See the Terms and Conditions (https://onlinelibrary.wiley.com/erms

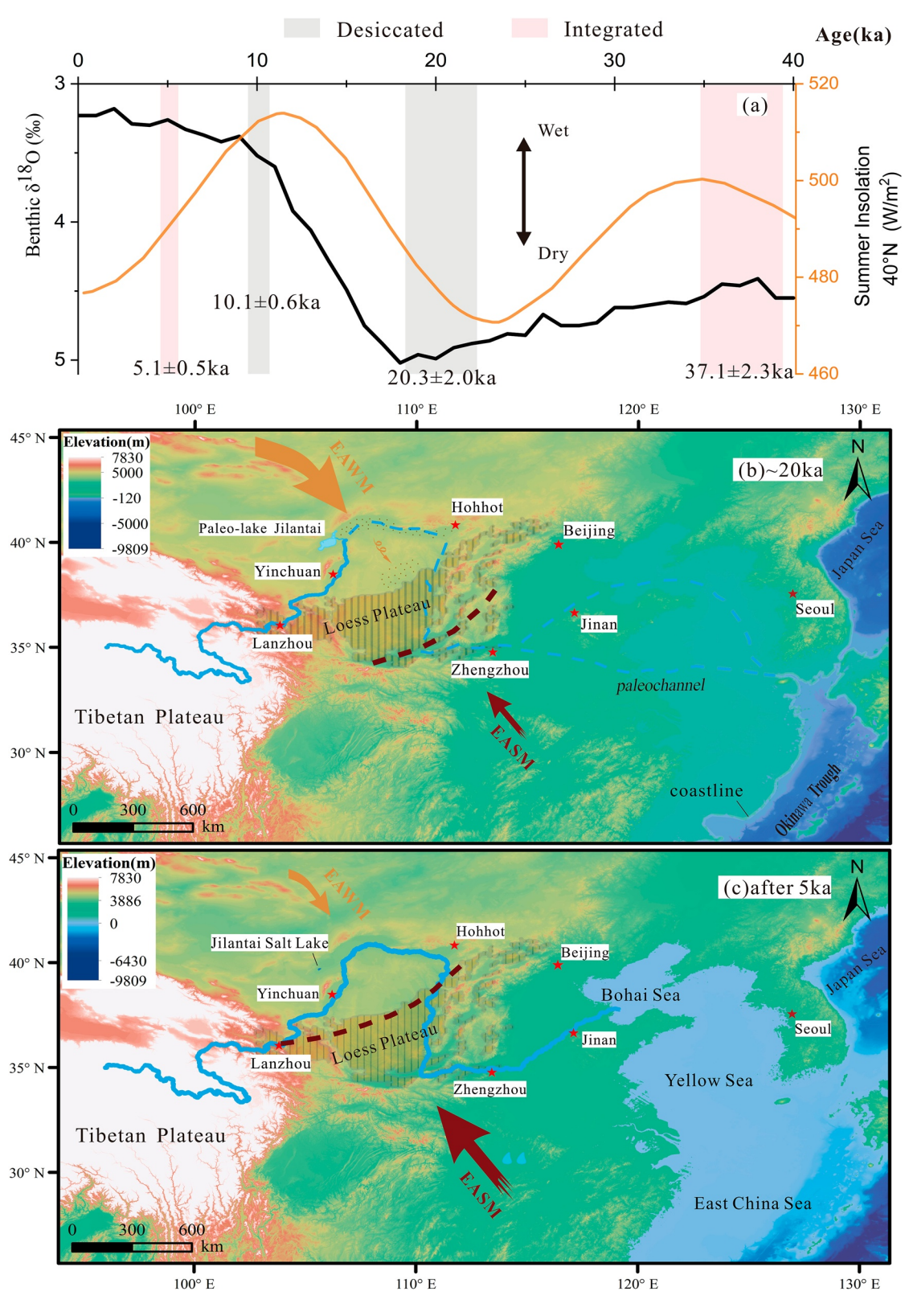


Figure 4.

ZHAO ET AL. 7 of 12

are governed by the applicable Creati

activity (M. Zhang, Liu, Yu, & Wang, 2022). Considering that enhanced sand dune formation can alter the flow path of river systems (B. Liu & Coulthard, 2015), we posit that the observed simultaneous paleo-lake highstand and enhanced regional aridity can be explained by diversion of the course of the upper Yellow River toward paleo-Lake Jilantai via sand barrier production (Figure 1b) (Tian et al., 2019) associated with lower Yellow River discharge (Figure 4b). When the regional climate became wetter during the early Holocene (11.8–5.6 ka), the salinity gradually increased, again supporting the interpretation that the water level variability of paleo-Lake Jilantai was mainly controlled by Yellow River water supply rather than local climatic oscillations.

The 87Sr/86Sr ratios, in combination with evaporite mineral content, indicate that the upper reaches of the Yellow River became desiccated during ~30–10 ka and that paleo-Lake Jilantai was the terminal lake. The reconstructed paleo-Lake Jilantai during the LGM, with an area of 5, 300 km² (Text S4 and Figure S7 in Supporting Information S1), was ~40 times larger than the modern Jilantai Salt Lake (120 km²), which is fed solely by local runoff. According to gauge data, the Yellow River has a mean annual water discharge of 2.6×10^{10} m³ near Jilantai today (Kong et al., 2016). Considering that (a) a lake with an area of 5, 300 km² could evaporate 8.16×10^9 m³ of water annually (Text S5 in Supporting Information S1), (b) colder intervals of the Pleistocene are associated with stronger near-surface winds and lower humidity (Abell et al., 2021; Beck et al., 2018; Y. Sun & An, 2005), and (c) less precipitation and meltwater runoff in the source regions of the Yellow River during the LGM likely resulted in reduced discharge (Huang et al., 2022; G. Li et al., 2015), there was potentially a balance between runoff into, and evaporation from, paleo-Lake Jilantai. As a result, little to no water from the Yellow River could flow out of the Hetao Basin, which is consistent with our geochemical data (detrital zircon geochronology and elemental geochemistry) from the Hequ terraces that suggest a proximal source dominated ~20-10 ka. Finally, provenance work on a drill core from the northern Okinawa Trough (Figure 4b) indicates that sediments deposited there were lacking materials from upsteam of the Yellow River during ~34–8 ka (Zhao et al., 2018), which may also suggest a lower runoff or desiccation in the upper reaches of the Yellow River.

4.3. A Novel Explanation for Variable Formation Ages of the Yellow River

By combining our provenance and geochemical results with existing lacustrine data, we demonstrate that the Yellow River experienced desiccation over the LGM and deglaciation. With that in mind, our interpretation that the Yellow River may have experienced periodic, climatically driven desiccation has several geological and geomorphological implications and, may be able to assist in resolving several debates regarding the formation age of the Yellow River.

The presence of large-scale desiccations and the subsequent re-establishment of flow may provide a possible clue for the divergent ages (e.g., 1.2 Ma [Jia et al., 2016; X. Wang et al., 2022], 880 ka [Yao et al., 2017], 120 ka [X. Zhang et al., 2018] or 12 ka [H. Yu, 1999]) proposed for the inception of the Yellow River (Q. Chen et al., 2022; Craddock et al., 2010; Xiao et al., 2020), with the periodic climate fluctuations since the mid-Pleistocene (An et al., 2015). Specifically, we suggest that each previously determined age may correspond to only one re-integration event, and the preceding or subsequent desiccation events were not considered because these studies assumed that a continental-scale river such as the Yellow River would remain integrated. While our proposed hypothesis regarding the inconsistent Yellow River formation ages is speculative and requires further revaluation, it provides a new framework for future dating studies dealing with the modern Yellow River's inception.

4.4. Implications for Terrestrial-Marine Source-To-Sink Processes

Our work highlights the importance of considering currently nonexistent desiccated riverbed sediments as potential dust sources for past periods of Earth's history. The erosion of the Chinese Loess Plateau was greatly

Figure 4. Climatic and hydrological changes of the Yellow River since the late Quaternary. (a) Desiccated and integrated states of the Yellow River, based on our data presented here, are shown as gray and pink bars, respectively. Variation in global marine benthic δ^{18} O values (Lisiecki & Raymo, 2005) and the calculated solar insolation at 40°N (J. Liu et al., 2019) since 40 ka are also displayed. (b) Regional schematic of Yellow River desiccation during the Last Glacial Maximum (LGM), when the paleo-Lake Jilantai was the terminal lake. Note the -120 m isobath representing the coastline during the LGM. The red triangle in the northern Okinawa Trough indicates IODP Site U1429 from Zhao et al. (2018). (c) Regional schematic of the integrated Yellow River and the contracted paleo-Lake Jilantai to the modern hyper-saline Jilantai Salt Lake after \sim 5 ka. The red dashed lines denote the East Asian Summer Monsoon margin varied with the coastline change from the LGM to mid-Holocene (Yang et al., 2015). The channel migrations in the plain downstream of Zhengzhou and the Hetao Basin are not fully considered.

ZHAO ET AL. 8 of 12

attenuated during times of lower runoff and without anthropogenic interference (Deng & Yuan, 2001; Sang et al., 2004), which could be explained by the desiccation of the upper Yellow River leading to (a) reduced sediment discharge farther downstream into the ocean during dry-cold periods, and (b) exposure of floodplains and lacustrine sediments that could act as sources for loess areas downwind (Nie et al., 2015). The aforementioned (as shown in Figure 2 and described in Section 4.1) climate-river desiccation feedbacks across glacial-interglacial cycles assist in better elucidating the source-to-sink relationship between the Chinese Loess Plateau and the Yellow River (Deng & Yuan, 2001; Peng et al., 2022). That is, despite the fact that Yellow River floodplains are not major sources of windblown detritus for the downwind North Pacific Ocean today (Zdanowicz et al., 2006), during glacial periods, these areas could be major dust sources due to persistent exposure to the air. Depending on the amount of exported material, this supposition might contrast with the traditional view that dust delivered to the North Pacific Ocean across a variety of timescales is primarily from Central and East Asian deserts active today (J. Sun et al., 2001; Yoon et al., 2019); a finding that is consistent with other studies from across Central and East Asia (Abell et al., 2020; Kapp et al., 2011; Pullen et al., 2011; D. Zhang et al., 2022). Overall, this is just another example that demonstrates how the use of modern conditions as a template to interpret past environments, while sometimes pertinent, may result in incorrect conclusions (Belanger et al., 2016; Nie et al., 2015; Stevens et al., 2010; Willenbring & Von Blanckenburg, 2010).

Taking a more global perspective, desiccation also occurred in the Nile River basin during the last glacial period (Abdelsalam, 2018; Box et al., 2011; Williams & Adamson, 1974). This finding, in combination with our new data for the Yellow River, suggests that climate-driven river desiccation on glacial-interglacial timescales, at least for the late Pleistocene (S. H. Liu et al., 2014), may be ubiquitous for arid-semiarid areas globally. Considering the described ramifications above for the Yellow River specifically, this process may play a substantial role in terrestrial-marine source-to-sink processes and the carbon cycle, as the soil carbon-atmosphere CO₂ flux induced by water erosion could be altered (Battin et al., 2023; Marx et al., 2017; Yue et al., 2016). In summary, while having been largely neglected by previous studies, the occurrence, timing, and role of major river desiccation should be considered in future studies.

Conflict of Interest

The authors declare no conflicts of interest relevant to this study.

Data Availability Statement

The authors declare that the data supporting the findings of this study are available within the paper and its supplementary files. The data on which this article is based are available in Fan et al. (2010), Licht et al. (2016), Lee et al. (2010), Nie et al. (2015), Pang et al. (2018), Stevens et al. (2013), J. Zhang et al. (2009), and M. Zhang, Liu, Yu, and Wang (2022). Supporting data of this study can be found at https://doi.org/10.6084/m9.figshare.23744652. The code based on the software Matlab to calculate the flexure deformation, water depth, etc., is available in its supplementary files and https://doi.org/10.6084/m9.figshare.23744652, and there is no restriction to access.

Acknowledgments This study was supported by the National Refere

Natural Science Foundation of China (51979179), the Second Tibetan Plateau Scientific Expedition and Research Program (2019QZKK0204), the Open Funding of State Key Laboratory of Loess and Quaternary Geology (2021LF1025) and Sichuan Science and Technology Program (2023NSFSC1989), J. T. A. is currently supported by a US NSF Division of Ocean Sciences Postdoctoral Fellowship (NSF-OCE-PRF 2126500). This work benefited from discussions with Martin Williams, Mengwei Zhang, Baotian Pan, Yuxin Fan, Guoqiang Li, Oinmian Xu, Fuqiang Li, Guoqiao Xiao, and Zhenbo Hu

References

Abdelsalam, M. (2018). The Nile's journey through space and time: A geological perspective. Earth-Science Reviews, 177, 742–773. https://doi.org/10.1016/j.earscirev.2018.01.010

Abell, J. T., Rahimi, S. R., Pullen, A., Lebo, Z. J., Zhang, D., Kapp, P., et al. (2020). A quantitative model-based assessment of stony desert landscape evolution in the Hami Basin, China: Implications for Plio-Pleistocene dust production in eastern Asia. *Geophysical Research Letters*, 47(20), e2020GL090064. https://doi.org/10.1029/2020gl090064

Abell, J. T., Winckler, G., Anderson, R. F., & Herbert, T. D. (2021). Poleward and weakened westerlies during Pliocene warmth. *Nature*, 589(7840), 70–75. https://doi.org/10.1038/s41586-020-03062-1

Amit, R., Enzel, Y., Mushkin, A., Gillespie, A., Batbaatar, J., Crouvi, O., et al. (2014). Linking coarse silt production in Asian sand deserts and Quaternary accretion of the Chinese Loess Plateau. *Geology*, 42(1), 23–26. https://doi.org/10.1130/g34857.1

An, Z., Wu, G., Li, J., Sun, Y., Liu, Y., Weijian, Z., et al. (2015). Global monsoon dynamics and climate change. *Annual Review of Earth and Planetary Sciences*, 43(1), 29–77. https://doi.org/10.1146/annurev-earth-060313-054623

Andersen, T., van Niekerk, H., & Elburg, M. A. (2022). Detrital zircon in an active sedimentary recycling system: Challenging the 'source-to-sink' approach to zircon-based provenance analysis. Sedimentology, 69(6), 2436–2462. https://doi.org/10.1111/sed.12996

Battin, T. J., Lauerwald, R., Bernhardt, E. S., Bertuzzo, E., Gener, L. G., Hall, R. O., Jr., et al. (2023). River ecosystem metabolism and carbon biogeochemistry in a changing world. *Nature*, 613(7944), 449–459. https://doi.org/10.1038/s41586-022-05500-8

ZHAO ET AL. 9 of 12

- Beck, J. W., Zhou, W., Li, C., Wu, Z., White, L., Xian, F., et al. (2018). A 550,000-year record of East Asian monsoon rainfall from ¹⁰Be in loess. Science, 360(6391), 877–881. https://doi.org/10.1126/science.aam5825
- Belanger, C. L., Orhun, O. G., & Schiller, C. M. (2016). Benthic foraminiferal faunas reveal transport dynamics and no-analog environments on a glaciated margin (Gulf of Alaska). *Palaeogeography, Palaeoclimatology, Palaeoecology*, 454, 54–64. https://doi.org/10.1016/j.palaeo.2016.04.032
- Box, M. R., Krom, M. D., Cliff, R. A., Bar-Matthews, M., Almogi-Labin, A., Ayalon, A., & Paterne, M. (2011). Response of the Nile and its catchment to millennial-scale climatic change since the LGM from Sr isotopes and major elements of East Mediterranean sediments. *Quaternary Science Reviews*, 30(3–4), 431–442. https://doi.org/10.1016/j.quascirev.2010.12.005
- Buylaert, J. P., Murray, A. S., Vandenberghe, D., Vriend, M., De Corte, F., & Van den haute, P. (2008). Optical dating of Chinese loess using sand-sized quartz: Establishing a time frame for Late Pleistocene climate changes in the western part of the Chinese Loess Plateau. *Quaternary Geochronology*, 3(1–2), 99–113. https://doi.org/10.1016/j.guageo.2007.05.003
- Chen, Q., Liu, X., Zhao, G., Jia, J., Ye, W., Lü, B., et al. (2022). 0.2 Ma or 1.2 Ma? Timing of the linking of the middle and lower reaches of the Yellow River inferred from loess-palaeosol sequences. *Geophysical Research Letters*, 49(6), e2021GL0975106. https://doi.org/10.1029/2021gl097510
- Chen, Y., Yan, M., Fang, X., Song, C., Zhang, W., Zan, J., et al. (2017). Detrital zircon U–Pb geochronological and sedimentological study of the Simao Basin, Yunnan: Implications for the Early Cenozoic evolution of the Red River. *Earth and Planetary Science Letters*, 476, 22–33. https://doi.org/10.1016/j.epsl.2017.07.025
- Craddock, W. H., Kirby, E., Harkins, N. W., Zhang, H., Shi, X., & Liu, J. (2010). Rapid fluvial incision along the Yellow River during headward basin integration. *Nature Geoscience*, 3(3), 209–213. https://doi.org/10.1038/ngeo777
- Deng, C., & Yuan, B. (2001). The gully erosion-accumulation process in the Loess Plateau of the middle Yellow River since the last interglacial period. *Journal of Geographical Sciences*, 1, 92–98. (in Chinese with English abstract).
- Dröllner, M., Barham, M., & Kirkland, C. L. (2022). Gaining from loss: Detrital zircon source-normalized a-dose discriminates first-versus multi-cycle grain histories. Earth and Planetary Science Letters, 579, 117346. https://doi.org/10.1016/j.epsl.2021.117346
- Fan, Y., Chen, F., Wei, G., Madsen, D., Oviatt, C., Zhao, H., et al. (2010). Potential water sources for late Quaternary Megalake Jilantai-Hetao, China, inferred from mollusk shell ⁸⁷Sr/⁸⁶Sr ratios. *Journal of Paleolimnology*, 43(3), 577–587. https://doi.org/10.1007/s10933-009-9353-4
- Fan, Y., Li, Z., Cai, Q., Yang, G., Zhang, Q., Zhao, H., et al. (2022). Dating of the late Quaternary high lake levels in the Jilantai area, north-western China, using optical luminescence of quartz and K-feldspar. *Journal of Asian Earth Sciences*, 224, 105024. https://doi.org/10.1016/j.iseaes.2021.105024
- Hou, M., Zhuang, G., Ji, J., Xiang, S., Kong, W., Cui, X., et al. (2021). Profiling interactions between the Westerlies and Asian summer monsoons since 45 ka: Insights from biomarker, isotope, and numerical modeling studies in the Qaidam Basin. Bulletin, 133(7–8), 1531–1541. https://doi.org/10.1130/b35751.1
- Hu, Z., Pan, B., Bridgland, D., Vandenberghe, J., Guo, L., Fan, Y., & Westaway, R. (2017). The linking of the upper-middle and lower reaches of the Yellow River as a result of fluvial entrenchment. *Quaternary Science Reviews*, 166, 324–338. https://doi.org/10.1016/j.quascirev.2017.02.026
- Huang, X., Lai, Z., Xu, L., Luo, L., Zhong, J., Xie, J., et al. (2022). Late Pleistocene lake overspill and drainage reversal in the source area of the Yellow River in the Tibetan Plateau. Earth and Planetary Science Letters, 589, 117554. https://doi.org/10.1016/j.epsl.2022.117554
- Jia, L., Zhang, X., Ye, P., Zhao, X., He, Z., He, X., et al. (2016). Development of the alluvial and lacustrine terraces on the northern margin of the Hetao Basin, Inner Mongolia, China: Implications for the evolution of the Yellow River in the Hetao area since the late Pleistocene. Geomorphology, 263, 87–98. https://doi.org/10.1016/j.geomorph.2016.03.034
- Kapp, P., Pelletier, J. D., Rohrmann, A., Heermance, R., Russell, J., & Ding, L. (2011). Wind erosion in the Qaidam basin, central Asia: Implications for tectonics, paleoclimate, and the source of the Loess Plateau. Geological Society of America Today, 21(4/5), 4–10. https://doi.org/10.1130/gsatg99a.1
- Kong, D., Miao, C., Wu, J., & Duan, Q. (2016). Impact assessment of climate change and human activities on net runoff in the Yellow River Basin from 1951 to 2012. *Ecological Engineering*, 91, 566–573. https://doi.org/10.1016/j.ecoleng.2016.02.023
- Kruskal, J. (1964). Multidimensional scaling by optimizing goodness of fit to a nonmetric hypothesis. Psychometrika, 29, 1–27. https://doi.org/10.1007/bf02289565
- Lee, M. K., Lee, Y. I., & Yi, H. I. (2010). Provenances of atmospheric dust over Korea from Sr–Nd isotopes and rare earth elements in early 2006. Atmospheric Environment, 44(20), 2401–2414. https://doi.org/10.1016/j.atmosenv.2010.04.010
- Li, G., Jin, M., Chen, X., Wen, L., Zhang, J., Madsen, D., et al. (2015). Environmental changes in the Ulan Buh Desert, southern Inner Mongolia, China since the middle Pleistocene based on sedimentology, chronology and proxy indexes. *Quaternary Science Reviews*, 128, 69–80. https://doi.org/10.1016/j.quascirev.2015.09.010
- Li, T., Li, J., & Zhang, D. D. (2020). Yellow River flooding during the past two millennia from historical documents. Progress in Physical Geography: Earth and Environment, 44(5), 661–678. https://doi.org/10.1177/0309133319899821
- Liang, H., Zhang, K., Fu, J., Li, L., Chen, J., Li, S., & Chen, L. (2015). Bedrock river incision response to basin connection along the Jinshan Gorge, Yellow River. North China. *Journal of Asian Earth Sciences*, 114, 203–211, https://doi.org/10.1016/j.iseaes.2015.07.010
- Licht, A., Pullen, A., Kapp, P., Abell, J., & Giesler, N. (2016). Eolian cannibalism: Reworked loess and fluvial sediment as the main sources of the Chinese Loess Plateau. GSA Bulletin, 128(5–6), 944–956. https://doi.org/10.1130/B31375.1
- Lisiecki, L., & Raymo, M. (2005). A Pliocene-Pleistocene stack of 57 globally distributed benthic δ¹⁸O records. Paleoceanography, 20(1), PA1003. https://doi.org/10.1029/2004pa001071
- Liu, B., & Coulthard, T. J. (2015). Mapping the interactions between rivers and sand dunes: Implications for fluvial and aeolian geomorphology. Geomorphology, 231, 246–257. https://doi.org/10.1016/j.geomorph.2014.12.011
- Liu, J., Wang, R., Zhao, Y., & Yang, Y. (2019). A 40,000-year record of aridity and dust activity at Lop Nur, Tarim Basin, northwestern China. Quaternary Science Reviews, 211, 208–221. https://doi.org/10.1016/j.quascirev.2019.03.023
- Liu, S. H., Feng, A. P., Du, J., Xia, D. X., Li, P., Xue, Z., et al. (2014). Evolution of the buried channel systems under the modern Yellow River delta since the Last Glacial Maximum. *Quaternary International*, 349, 327–338. https://doi.org/10.1016/j.quaint.2014.06.061
- Ma, H., Nittrouer, J. A., Fu, X., Parker, G., Zhang, Y., Wang, Y., et al. (2022). Amplification of downstream flood stage due to damming of fine-grained rivers. *Nature Communications*, 13(1), 3054. https://doi.org/10.1038/s41467-022-30730-9
- Marx, A., Dusek, J., Jankovec, J., Sanda, M., Vogel, T., van Geldern, R., et al. (2017). A review of CO₂ and associated carbon dynamics in headwater streams: A global perspective. *Reviews of Geophysics*, 55(2), 560–585. https://doi.org/10.1002/2016rg000547
- McGee, D. (2020). Glacial-interglacial precipitation changes. Annual Review of Marine Science, 12(1), 525–557. https://doi.org/10.1146/annurev-marine-010419-010859
- Medialdea, A., Thomsen, K. J., Murray, A. S., & Benito, G. (2014). Reliability of equivalent-dose determination and age-models in the OSL dating of historical and modern palaeoflood sediments. *Quaternary Geochronology*, 22, 11–24. https://doi.org/10.1016/j.quageo.2014.01.004

ZHAO ET AL. 10 of 12

- Nie, J., Stevens, T., Rittner, M., Stockli, D., Garzanti, E., Limonta, M., et al. (2015). Loess plateau storage of northeastern Tibetan plateau-derived Yellow River sediment. *Nature Communications*, 6(1), 1–10. https://doi.org/10.1038/ncomms9511
- Pang, H., Pan, B., Garzanti, E., Gao, H., Zhao, X., & Chen, D. (2018). Mineralogy and geochemistry of modern Yellow River sediments: Implications for weathering and provenance. Chemical Geology, 488, 76–86. https://doi.org/10.1016/j.chemgeo.2018.04.010
- Peng, F., Nie, J., Stevens, T., & Pan, B. (2022). Decoupled Chinese Loess Plateau dust deposition and Asian aridification at millennial and tens of millennial timescales. Geophysical Research Letters, 49(20), e2022GL099338. https://doi.org/10.1029/2022gl099338
- Pullen, A., Kapp, P., McCallister, A. T., Chang, H., Gehrels, G. E., Garzione, C. N., et al. (2011). Qaidam Basin and northern Tibetan Plateau as dust sources for the Chinese Loess Plateau and paleoclimatic implications. Geology, 39(11), 1031–1034. https://doi.org/10.1130/g32296.1
- Qian, Y., Wu, Z., Shi, J., Wu, Z., & Jin, J. (1993). Characteristics and sources of material composition in the Taklimakan Desert. *China Desert*, 13(4), 32–38. (in Chinese with English abstract).
- Sang, G. (2004). Research progress on historical geomorphology and soil erosion evolution of the Loess Plateau. *Journal of Zhejiang Normal University (Natural Sciences)*, 04, 78–82. (in Chinese with English abstract).
- Saylor, J. E., Jordan, J. C., Sundell, K. E., Wang, X., Wang, S., & Deng, T. (2018). Topographic growth of the Jishi Shan and its impact on basin and hydrology evolution, NE Tibetan Plateau. *Basin Research*, 30(3), 544–563. https://doi.org/10.1111/bre.12264
- Stevens, T., Carter, A., Watson, T. P., Vermeesch, P., Andò, S., Bird, A., et al. (2013). Genetic linkage between the Yellow River, the Mu Us desert, and the Chinese Loess Plateau. *Quaternary Science Reviews*, 78, 355–368. https://doi.org/10.1016/j.quascirev.2012.11.032
- Stevens, T., Palk, C., Carter, A., Lu, H., & Clift, P. D. (2010). Assessing the provenance of loess and desert sediments in northern China using U-Pb dating and morphology of detrital zircons. *Bulletin*, 122(7–8), 1331–1344. https://doi.org/10.1130/b30102.1
- Sun, J., Zhang, M., & Liu, T. (2001). Spatial and temporal characteristics of dust storms in China and its surrounding regions, 1960–1999: Relations to source area and climate. *Journal of Geophysical Research: Atmospheres*, 106(D10), 10325–10333, https://doi.org/10.1029/2000id900665
- to source area and climate. *Journal of Geophysical Research: Atmospheres, 106*(D10), 10325–10333. https://doi.org/10.1029/2000jd900665 Sun, Y., & An, Z. (2005). Late Pliocene-Pleistocene changes in mass accumulation rates of eolian deposits on the central Chinese Loess Plateau.
- Journal of Geophysical Research: Atmospheres, 110, D23. https://doi.org/10.1029/2005jd006064
 Sundell, K. E., & Saylor, J. E. (2017). Unmixing detrital geochronology age distributions. Geochemistry, Geophysics, Geosystems, 18(8), 2872–
- 2886. https://doi.org/10.1002/2016gc006774
- Tang, H., Gao, M., Yuan, S., Zhang, H., Xiao, Y., Zhang, F., & Zhang, K. (2023). Impact of the Yellow River capture on the paleoenvironmental changes of Hongze Lake, China. International Journal of Sediment Research, 38(4), 503–515. https://doi.org/10.1016/j.ijsrc.2023.02.002
- Tian, S., Yu, G., Jiang, E., Guo, J., Li, Z., & Wang, Y. (2019). Reevaluation of the aeolian sand flux from the Ulan Buh Desert into the upper Yellow River based on in situ monitoring. *Geomorphology*, 327, 307–318. https://doi.org/10.1016/j.geomorph.2018.11.009
- Wang, X., Hu, G., Saito, Y., Ni, G., Hu, H., Yu, Z., et al. (2022). Did the modern Yellow River form at the Mid-Pleistocene transition? *Science Bulletin*, 67(15), 1603–1610. https://doi.org/10.1016/j.scib.2022.06.003
- Wang, Z., Zhou, H., Wang, X., & Jing, X. (2015). Characteristics of the crystalline basement beneath the Ordos Basin: Constraint from aeromag-
- netic data. Geoscience Frontiers, 6(3), 465–475. https://doi.org/10.1016/j.gsf.2014.02.004
 Willenbring, J. K., & Von Blanckenburg, F. (2010). Long-term stability of global erosion rates and weathering during late-Cenozoic cooling.
- Nature, 465(7295), 211–214. https://doi.org/10.1038/nature09044
 Williams, M., & Adamson, D. (1974). Late Pleistocene desiccation along the White Nile. Nature, 248(5449), 584–586. https://doi.org/10.1038/248584a0
- Wu, Y., Fang, X., Liao, S., Xue, L., Chen, Z., Yang, J., et al. (2020). Crustal evolution events in the Chinese continent: Evidence from a zircon U-Pb database. *International Journal of Digital Earth*, 13(12), 1532–1552. https://doi.org/10.1080/17538947.2020.1739152
- Xia, D., Liu, Z., Wu, S., & Cui, J. (1996). Preliminary study on the disintegration of the Yellow River during the last glacial period. *Ocean and Limnology*, 5, 511–517. (in Chinese with English abstract).
- Ziao, G., Sun, Y., Yang, J., Yin, Q., Dupont-Nivet, G., Licht, A., et al. (2020). Early Pleistocene integration of the Yellow River I: Detrital-zircon evidence from the North China Plain. *Palaeogeography, Palaeoclimatology, Palaeoecology*, 546, 109691. https://doi.org/10.1016/j.
- Yan, D., & Bernd, W. (2014). Late Quaternary water depth changes in Hala Lake, northeastern Tibetan Plateau, derived from ostracod assemblages and sediment properties in multiple sediment records. *Quaternary Science Reviews*, 95, 95–114. https://doi.org/10.1016/j. quascirey.2014.04.030
- Yang, S., Ding, Z., Li, Y., Wang, X., Jiang, W., & Huang, X. (2015). Warming-induced northwestward migration of the East Asian monsoon rain belt from the Last Glacial Maximum to the mid-Holocene. *Proceedings of the National Academy of Sciences*, 112(43), 13178–13183. https://doi.org/10.1073/pnas.1504688112
- Yao, Z., Shi, X., Qiao, S., Liu, Q., Kandasamy, S., Liu, J., et al. (2017). Persistent effects of the Yellow River on the Chinese marginal seas began at least ~880 ka ago. Scientific Reports, 7(1), 1–11. https://doi.org/10.1038/s41598-017-03140-x
- Yoon, J. E., Lim, J. H., Shim, J. M., Kwon, J. I., & Kim, I. N. (2019). Spring 2018 Asian Dust Events: Sources, transportation, and potential biogeochemical implications. *Atmosphere*, 10(5), 276. https://doi.org/10.3390/atmos10050276
- Yu, H. (1999). Ages of the Yellow River delta in shelf regions of the Yellow Sea and the Bohai Sea. *Journal of Geomechanics*, 4, 82–90. (in Chinese with English abstract).
- Yu, S., Hou, Z., Chen, X., Wang, Y., Song, Y., Gao, M., et al. (2020). Extreme flooding of the lower Yellow River near the Northgrippian-Meghalayan boundary: Evidence from the Shilipu archaeological site in southwestern Shandong Province, China. Geomorphology, 350, 106878. https://doi.org/10.1016/j.geomorph.2019.106878
- Yu, S., Zheng, Z., Chen, F., Jing, X., Kershaw, P., Moss, P., et al. (2017). A last glacial and deglacial pollen record from the northern South China Sea: New insight into coastal-shelf paleoenvironment. *Quaternary Science Reviews*, 157, 114–128. https://doi.org/10.1016/j. quascirev.2016.12.012
- Yue, Y., Ni, J., Ciais, P., Piao, S., Wang, T., Huang, M., et al. (2016). Lateral transport of soil carbon and land–atmosphere CO₂ flux induced by water erosion in China. *Proceedings of the National Academy of Sciences*, 113(24), 6617–6622. https://doi.org/10.1073/pnas.1523358113
- Zdanowicz, C., Hall, G., Vaive, J., Amelin, Y., Percival, J., Girard, I., et al. (2006). Asian dustfall in the St. Elias Mountains, Yukon, Canada. Geochimica et Cosmochimica Acta, 70(14), 3493–3507. https://doi.org/10.1016/j.gca.2006.05.005
- Zhang, D., Wang, G., Abell, J. T., Pullen, A., Winckler, G., Schaefer, J. M., & Shen, T. (2022). Quantifying late Pleistocene to Holocene erosion rates in the Hami Basin, China: Insights into Pleistocene dust dynamics of an East Asian stony desert. *Geophysical Research Letters*, 49(8), e2021GL097495. https://doi.org/10.1029/2021gl097495
- Zhang, J., Qiu, W., Li, R., & Zhou, L. (2009). The evolution of a terrace sequence along the Yellow River (HuangHe) in Hequ, Shanxi, China, as inferred from optical dating. *Geomorphology*, 109(1–2), 54–65. https://doi.org/10.1016/j.geomorph.2008.08.024
- Zhang, M., Liu, X., Yu, Z., & Wang, Y. (2022). Paleolake evolution in response to climate change since middle MIS 3 inferred from Jilantai Salt Lake in the marginal regions of the ASM domain. *Quaternary International*, 607, 48–57. https://doi.org/10.1016/j.quaint.2021.06.017

ZHAO ET AL. 11 of 12

- Zhang, R., Cao, J., Tang, Y., Arimoto, R., Shen, Z., Wu, F., et al. (2014). Elemental profiles and signatures of fugitive dusts from Chinese deserts. Science of the Total Environment, 472, 1121–1129. https://doi.org/10.1016/j.scitotenv.2013.11.011
- Zhang, X., Liu, Y., Wang, S., Liu, W., & Xue, W. (2018). On the chronology of the Yellow Rivers and the Yangtze Rivers. *Mountain Research*, 36(5), 661–668. (in Chinese with English abstract).
- Zhao, D., Wan, S., Clift, P. D., Tada, R., Huang, J., Yin, X., et al. (2018). Provenance, sea-level and monsoon climate controls on silicate weathering of Yellow River sediment in the northern Okinawa Trough during late last glaciation. *Palaeogeography, Palaeoclimatology, Palaeoecology*, 490, 227–239. https://doi.org/10.1016/j.palaeo.2017.11.002

References From the Supporting Information

- Chen, F., Fan, Y., Chun, X., Madsen, D. B., Oviatt, C. G., Zhao, H., et al. (2008). Preliminary study on the late Quaternary Jilantai-Hetao Megalake. Chinese Science Bulletin, 10, 1207–1219. (in Chinese with English abstract).
- Ding, L., Yang, D., Cai, F. L., Pullen, A., Kapp, P., Gehrels, G. E., et al. (2013). Provenance analysis of the Mesozoic Hoh-Xil-Songpan-Ganzi turbidites in northern Tibet: Implications for the tectonic evolution of the eastern Paleo-Tethys Ocean. *Tectonics*, 32(1), 34–48. https://doi. org/10.1002/tect.20013
- Gartmair, G., Barham, M., & Kirkland, C. L. (2023). One size does not fit all: Refining zircon provenance interpretations via integrated grain shape, geochronology, and Hf isotope analysis. *Geoscience Frontiers*, 14(4), 101579. https://doi.org/10.1016/j.gsf.2023.101579
- Gehrels, G. E., Yin, A., & Wang, X. F. (2003). Magmatic history of the northeastern Tibetan Plateau. Journal of Geophysical Research: Solid Earth, 108(B9). https://doi.org/10.1029/2002jb001876
- Jackson, E., Pearson, J., Griffin, L., & Belousova, A. (2004). The application of laser ablation-inductively coupled plasma-mass spectrometry to in situ U-Pb zircon geochronology. Chemical Geology, 211(1-2), 47-69. https://doi.org/10.1016/j.chemgeo.2004.06.017
- Jordan, T., & Watts, A. (2005). Gravity anomalies, flexure and the elastic thickness structure of the India–Eurasia collisional system. *Earth and Planetary Science Letters*, 236(3–4), 732–750. https://doi.org/10.1016/j.epsl.2005.05.036
- Li, G., Wang, Z., Zhao, W., Jin, M., Wang, X., Tao, S., et al. (2020). Quantitative precipitation reconstructions from Chagan Nur revealed lag response of East Asian summer monsoon precipitation to summer insolation during the Holocene in arid northern China. Quaternary Science Reviews, 239, 106365. https://doi.org/10.1016/j.quascirev.2020.106365
- Shi, X., Furlong, K. P., Kirby, E., Meng, K., Marrero, S., Gosse, J., et al. (2017). Evaluating the size and extent of paleolakes in central Tibet during the late Pleistocene. *Geophysical Research Letters*, 44(11), 5476–5485. https://doi.org/10.1002/2017gl072686
- Sláma, J., & Košler, J. (2012). Effects of sampling and mineral separation on accuracy of detrital zircon studies. Geochemistry, Geophysics, Geosystems, 13, Q05007. https://doi.org/10.1029/2012GC004106
- Sun, F., Hu, W., Cao, J., Wang, X., Zhang, Z., Ramezani, J., & Shen, S. (2022). Sustained and intensified lacustrine methane cycling during Early Permian climate warming. *Nature Communications*, 13(1), 4856. https://doi.org/10.1038/s41467-022-32438-2
- Wang, L., Chen, X., & Chu, T. (1997). Comparative analysis of sediment characteristics in Yellow River and Yangtze River. *Geographical Research*, 16(4), 71–79. (in Chinese with English abstract).

ZHAO ET AL. 12 of 12